Novel Interconnect Modeling by Using High-Order Compact Finite Difference Methods

Qinwei Xu and Pinaki Mazumder
EECS Dept., University of Michigan, Ann Arbor, MI 48109
email: {qwxu,mazum}@eecs.umich.edu

Abstract— **The high-order compact finite difference (HCFD) method is adapted for interconnect modeling. Based on the compact finite difference method, the HCFD method employs the Chebyshev polynomials to construct the approximation framework for interconnect discretization, and leads to improved equivalent-circuit models. The HCFD-based modeling requires far fewer intervening grid points for building an accurate discrete model of the transmission line than other numerical methods like traditional Finite Difference (FD) method. It is believed that given the number of state variables, the presented method gives more accurate results than other known passive discrete modeling methods. The theoretical proof shows that HCFD-based modeling preserves the passivity.**

I. Introduction

The integrated circuits and systems fabricated in the forms of multi-chip modules (MCMs) and system-on-chips (SOCs) have become both larger in chip area and faster in operation. As interconnections usually have large size, heavy density, and high order of RLCG circuit elements, reduced order modeling approaches have been employed for efficient circuit simulation. Asymptotic Waveform Evaluation (AWE) and its extensions are the most well-known methods for the approximation of general linear networks [1], [2]. The Krylov subspace techniques have been afterwards developed addressing the issue of passivity giving rise to efficient passive reduced order algorithms [3]. On the other hand, the congruence transformations have been successfully applied to reduced-order modeling [4]. An extended technique based on Arnoldi's method with congruence transformations is presented in the literature [5], in which the PRIMA algorithm was demonstrated as an effective approach for developing passive reduced-order models.

Although the algorithms of model reductions are well developed, they can only handle the finite order systems in the forms of state equations. Interconnects, however, are governed by nonlinear partial differential equations, which are actually infinite order systems. Therefore, it is inevitable to represent the interconnects with approximate models involving finite state variables prior to further model reduction. In order to efficiently perform the reduction algorithms on the finite system, the interconnect modeling needs to involve as few state variables as possible, while retaining required accuracy. Most effort to develop finite order models of distributed interconnect is focused on direct discretization approaches, which generally select grid points along the lines. Since the finite difference (FD) methods was already applied to the interconnect problems, the discretization of interconnects has been well known. Despite its simplicity, it has, however, the disadvantage that the number of grid points, depending on the minimum wavelength, is generally very large. Consequently, such an approach results in very large numbers of lumped elements for accurate modeling and thus sharply increase the number of state variables of the whole circuit. This problem becomes severely worse when tackling the 3-D interconnect structures. A compact difference method with the fourth order accuracy is employed in the literature [6]. In this discretization approach, the number of unknowns per wavelength required for highly accurate modeling is smaller and its dependence on the electrical length of the line is weaker.

The drawback of low order finite methods can be overcome by using the high order finite methods or pseudospectral methods [7]. Based on the same kind of mathematical fundamental, the scheme of low order finite method is determined by low order Taylor series, while the scheme of high order finite method is determined by high order Taylor series. The advantage of high order schemes is twofold: they allow one either to increase accuracy while keeping the number of mesh points fixed or to reduce the computational cost by decreasing the grid dimension while preserving accuracy. In general, the high order schemes have a high order truncation error. Thus, to achieve required accuracy, the grid points used by the high order schemes can be much sparser than those used

This work was partially supported by ONR grant under the Dual-Use Program.

by low order schemes. As a result, the high order schemes can obtain accurate numerical solutions using very few mesh points. Chebyshev polynomial representation, a kind of pseudospectral methods, has been used to model interconnects and has shown high efficiency [8]. However, it cannot guarantee passivity.

In this paper, the high-order compact finite difference (HCFD) method is presented for passive modeling of interconnects. Based on the concept of compact finite difference method, the HCFD approximation frame is constructed over all the grid points of the interconnects, and the coefficients of the approximation frame are calculated by using the Chebyshev polynomials. The HCFD method is more flexible than other compact finite difference methods in that it can achieve N-th order approximation, where N is the number of the grid points, compared to the known compact finite difference methods which have a fixed order of approximation (e.g., 4-th order in [9]). This paper develops in the following steps. At first, the global approximations are reviewed and then the specific approximation frames of the HCFD method are constructed. The discrete modeling are derived by using the HCFD-based approximation frames, and the equivalent circuit models are consequently obtained. The HCFD-based modeling is proved to guarantee passivity. Like FD-based models, the HCFD-based discrete models can be incorporated into popular all-purpose simulators. Due to the global approximation, given the number of the grid points, the presented discrete modeling is believed to yield higher approximation accuracy than any other discrete modeling does.

II. High-order compact finite difference method

In the following discussion, we assume that for a single RLCG interconnect, the governing Telegrapher's equations are

$$\begin{aligned}\frac{d}{dx}V(x,s) &= -(sL+R)I(x,s)\\ \frac{d}{dx}I(x,s) &= -(sC+G)V(x,s). \end{aligned} \quad (1)$$

where the length of the single interconnect has been normalized as $[0,1]$, and

$$Z(s) = (R+sL) \quad (2)$$

$$Y(s) = (G+sC) \quad (3)$$

Segmenting the interconnect with one unit length into $2N$ sections, each section has the length $h = 0.5/N$. Define the voltage grid set:

$$\{u_0 = 0, u_i = (2i-1)h, i = 1,\ldots,N, u_{N+1} = 1\}, \quad (4)$$

and the current grid set:

$$\{v_i = 2(i-1)h, i = 1,\ldots,N+1\}, \quad (5)$$

as shown in Fig. 1.

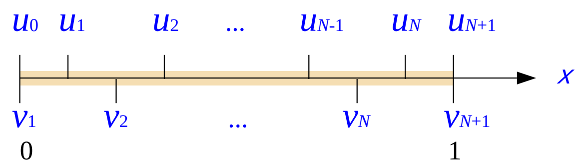

Fig. 1. Approximation framework.

Along the line, are distributed the continuous voltage $V(x)$ and current $I(x)$ (for simplicity, the distributed voltage $V(x,s)$ and current $I(x,s)$ are written as $V(x)$ and $I(x)$ where no confusion caused). By analogy to the compact finite difference method [9], the approximation frames at the voltage grid points and at the current grid points are, respectively:

$$V(u_{k+1}) - V(u_k) = \sum_{j=1}^{N+1} a_{kj}\frac{d}{dx}V(x)|_{x=v_j} \quad (6)$$

$$I(v_{k+1}) - I(v_k) = \sum_{j=1}^{N} b_{kj}\frac{d}{dx}I(x)|_{x=u_j} \quad (7)$$

where a_{ij}'s and b_{ij}'s are to be determined by using the Chebyshev polynomials as test functions:

$$\begin{aligned} T_0(x) &= 1\\ T_1(x) &= x\\ T_2(x) &= 2x^2-1\\ &\ldots\\ T_n(x) &= 2xT_{n-1}(x) - T_{n-2}(x) \end{aligned} \quad (8)$$

For each k, we substitute an appropriate number of Chebyshev polynomials from $T_0(x)$ to $T_n(x)$ into Eqn. 6, then a set of $(N+1)\times(N+1)$ linear equations are obtained, with $\{a_{k1}, a_{k2}, \ldots, a_{k(N+1)}\}$ being the unknowns. The coefficients can be obtained by solving the obtained linear equations. The coefficients $\{b_{k1}, b_{k2}, \ldots, b_{kN}\}$ can be calculated by the similar way.

In the process to calculate the two coefficient matrices $\mathbf{A} = \{a_{ij}\}$ and $\mathbf{B} = \{b_{ij}\}$, not all the coefficients are independent: some coefficients have higher priority to be determined, and the others will be determined by the previously determined ones. Three rules for the priority are followed.

Rule 1: Central priority. Among those undetermined coefficients, compute first the coefficient $\{a_{kj}\}$ and $\{b_{kj}\}$ whose k's are closest to $\lceil N/2 \rceil$ (the ceiling of $N/2$).

Rule 2: Passive symmetry. The symmetry of the coefficient matrices $\{a_{ij}\}$ and $\{b_{ij}\}$ are forced, which leads to $a_{ij} = a_{ji}$ and $b_{ij} = b_{ji}$.

Rule 3: Structural symmetry. Because the grid points are geometrically symmetrical with respect to the mid-point, the coefficient matrices are symmetrical with respect to the secondary diagonal, i.e., $a_{ij} = a_{(N-i+1)(N-j+1)}$ and $b_{ij} = a_{(N-i)(N-j)}$. Note that this symmetry is a natural results of Rules 1 and 2, as long as the grid points are uniformly distributed.

For example of $\{a_{kj}\}$, this *algorithm* can be described as follows:

While (There are undetermined $\{a_{kj}\}$*'s)* $\{$
Select k and Eqns. 6 and 7 according to *Rule 1*.
Substitute Eqns. 8 into the selected equations.
Form a set of linear equations.
Solve the equations to obtain $\{a_{kj}\}$'s.
Apply *Rule 2*.
Apply *Rule 3*.
$\}$

Depending on the different number of Chebyshev polynomials employed to determine the coefficients, the approximation at different grid points has different accuracy. According to the above algorithm, the approximation at the midpoint of the interconnect has the highest accuracy (N-th order), and the accuracy decreases in the directions to both boundaries. As a result of the algorithm, we have the following Lemma:

Lemma 0: The coefficient matrices $\mathbf{A}$ and $\mathbf{B}$ determined by using Eqns. 6 and 7 under the rules 1-3 are non-negative, symmetric and real matrices.

For simplicity, denote $V_i = V(u_i), i = 0, \ldots, N+1$ and $I_i = I(v_i), i = 1, \ldots, N+1$. From Eqns. 6 and 7, we obtain the discrete modeling approximation:

$$\begin{bmatrix} V_1 - V_0 \\ V_2 - V_1 \\ \vdots \\ V_{N+1} - V_N \end{bmatrix} = -Z(s)\mathbf{A} \begin{bmatrix} I_1 \\ I_2 \\ \vdots \\ I_{N+1} \end{bmatrix} \tag{9}$$

$$\begin{bmatrix} I_2 - I_1 \\ I_3 - I_2 \vdots \\ I_{N+1} - I_N \end{bmatrix} = -Y(s)\mathbf{B} \begin{bmatrix} V_1 \\ V_2 \\ \vdots \\ V_N \end{bmatrix} \tag{10}$$

where

$$\mathbf{A} = \begin{bmatrix} a_{11} & \ldots & a_{1(N+1)} \\ & \ddots & \\ a_{(N+1)1} & \ldots & a_{(N+1)(N+1)} \end{bmatrix} \tag{11}$$

$$\mathbf{B} = \begin{bmatrix} b_{11} & \ldots & b_{1N} \\ & \ddots & \\ b_{N1} & \ldots & b_{NN} \end{bmatrix} \tag{12}$$

Eqns. 9 and 10 apparently have the full globality, because the approximation is represented by the values distributed in the entire domain. The local approximations like FD method use up to second order polynomials to determine the coefficients, leading to the accuracy of at best second order. The global approximations in Eqns. 9 and 10 use up to N-th order Chebyshev polynomials to determine the approximation frame, which is the highest order in this case; therefore, this method is called high-order compact finite difference (HCFD). The HCFD method achieves the best accuracy at the midpoint, and better accuracy at other points than semi-global or local approximations.

One may notice that the drawback of the HCFD method is that it generates the dense matrices (Eqns. 11 and 12), compared to the sparse matrices generated by FD methods. If these matrices have very large scale, the computational complexity will become worse than that of parse matrices. However, the dimension of the matrices are generally small. As shown in the numerical experiments, $N = 2$ or $N = 3$ per minimum wavelength can already give considerably accurate results. In this sense, the small dense matrices in this method have advantage over the large sparse matrices.

III. Equivalent Circuit Model

Defining the current controlled voltage sources (CCVS) and the voltage controlled current sources (VCCS) by

$$V_i^e = Z(s) \sum_{j=1}^{N+1} a_{ij} I_j \tag{13}$$

where $i = 1, \ldots, N+1; j = 1, \ldots, N$.

$$I_i^e = Y(s) \sum_{j=1}^{N} b_{ij} V_j \tag{14}$$

where $i = 2, \ldots, N+1; j = 1, \ldots, N$. Then the equivalent circuit of the discrete model can be schematically represented by Fig. 2.

Fig. 2 shows that this discrete modeling has explicit physical meaning. The discrete model consists of a chain of current controlled voltage sources (CCVS) and voltage controlled current sources (VCCS), compared to the FD-based discrete model consisting of a cascade of RLC elements. In Eqns. 13 and 14, every equivalent voltage/current source in the equivalent circuit is contributed

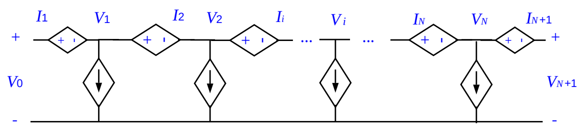

Fig. 2. Equivalent discrete model.

by all of the other current/voltage state variables. The global approximations improve the accuracy by reducing the truncate error to up to h^N [10].

It is well known that the passivity of the interconnect modeling is extremely important to guarantee the stability as well as accuracy. In order to do this, the following definitions and results [11] are used.

Lemma 1: Necessary and sufficient conditions for a transfer function $n \times n$ matrix $\mathbf{Y}(s)$ to be passive (i.e., $\mathbf{Y}(s)$ is positive-real) are given by:
(1) each element of $\mathbf{Y}(s)$ is analytic in $\Re(s) > 0$,
(2) $\mathbf{Y}(s^*) = \mathbf{Y}^*(s)$ and
(3) $(\mathbf{Y}^*)^T(s) + \mathbf{Y}(s)$ is non-negative definite for all $\Re(s) \geq 0$.

Lemma 2: An n-port network is passive if and only if its admittance matrix $\mathbf{Y}(s)$ is positive-real.

Lemma 3: If $\mathbf{C}(s)$ is positive-real, then $\mathbf{C}^{-1}(s)$ is positive-real, if it exists.

Lemma 4: If $\mathbf{C}(s)$ is positive-real and $\mathbf{D}$ is real, then $\mathbf{D}^T\mathbf{C}(s)\mathbf{D}$ is positive-real.

If two independent voltage excitations are connected to V_0 and V_{N+1}, respectively, the state equation of the discrete model shown in Fig. 2 can be formulated by using the modified nodal analysis (MNA):

$$\begin{bmatrix} \mathbf{P}_1 + s\mathbf{Q}_1 & \mathbf{P}_3 \\ -\mathbf{P}_3^T & \mathbf{P}_2 + s\mathbf{Q}_2 \end{bmatrix} \begin{bmatrix} \mathbf{V} \\ \mathbf{I} \end{bmatrix} = \mathbf{D}_i \tag{15}$$

where

$$\begin{aligned} \mathbf{P}_1 + s\mathbf{Q}_1 &= Y(s)\mathbf{B} \\ \mathbf{P}_2 + s\mathbf{Q}_2 &= Z(s)\mathbf{A} \\ \mathbf{P}_3 &= \begin{bmatrix} -1 & 1 & & \\ & \ddots & \ddots & \\ & & -1 & 1 \end{bmatrix} \end{aligned}$$

$\mathbf{V} = [V_1\ V_2\ \ldots\ V_N]^T \in R^N$ is the vector of nodal voltages;

$\mathbf{I} = [I_1\ I_2\ \ldots\ I_{N+1}]^T \in R^{N+1}$ is the vector of branch currents;

the matrices $\mathbf{P}_1$, $\mathbf{P}_2$, $\mathbf{P}_3$, $\mathbf{Q}_1$ and $\mathbf{Q}_2$ are derived from Eqn. 15:

$\mathbf{P}_1 \in R^{N\times N}$ and $\mathbf{P}_2 \in R^{(N+1)\times(N+1)}$ are symmetric and nonnegative definite, having units of conductance and resistance, respectively;

$\mathbf{Q}_1 \in R^{N\times N}$ and $\mathbf{Q}_2 \in R^{(N+1)\times(N+1)}$ are symmetric and nonnegative definite, having units of capacitance and inductance, respectively;

$\mathbf{P}_3 \in R^{N\times(N+1)}$, connecting matrix, is comprised of 1 or 0.

The matrix $\mathbf{D}_i \in R^{2N+1}$ contains two independent voltage sources connected to the two ends of interconnect, which can be represented as

$$\mathbf{D}_i = \begin{bmatrix} 0 & \ldots & 0 & 1 & \ldots & 0 \\ 0 & \ldots & 0 & 0 & \ldots & -1 \end{bmatrix}^T \begin{bmatrix} V_0^s \\ V_{N+1}^s \end{bmatrix} = \mathbf{D}\mathbf{V}^s \tag{16}$$

Noting that the original port variables are V_0, I_1, V_{N+1} and $-I_{N+1}$, the admittance matrix is obtained as:

$$\mathbf{Y}(s) = \mathbf{D}^T \begin{bmatrix} \mathbf{P}_1 + s\mathbf{Q}_1 & \mathbf{P}_3 \\ -\mathbf{P}_3^T & \mathbf{P}_2 + s\mathbf{Q}_2 \end{bmatrix}^{-1} \mathbf{D} \tag{17}$$

Theorem : The matrix $\mathbf{Y}(s)$ in Eqn. 17 is positive-real.

Proof: Using Lemmas 1-4, the matrix $\mathbf{Y}(s)$ being positive-real ascribes to that the following matrix is positive-real:

$$\mathbf{W} = \begin{bmatrix} \mathbf{P}_1 + s\mathbf{Q}_1 & \mathbf{P}_3 \\ -\mathbf{P}_3^T & \mathbf{P}_2 + s\mathbf{Q}_2 \end{bmatrix}. \tag{18}$$

Referring back to Lemma 1, the first two conditions are automatically satisfied for matrix $\mathbf{W}$. In proving that matrix $\mathbf{W}$ satisfies condition (3), noting that matrices $\mathbf{P}_1$, $\mathbf{P}_2$, $\mathbf{Q}_1$ and $\mathbf{Q}_2$ are all symmetric, which is guaranteed by *Lemma 0*, therefore,

$$\mathbf{W} + (\mathbf{W}^*)^T = 2\begin{bmatrix} \mathbf{P}_1 + \sigma\mathbf{Q}_1 & \mathbf{0} \\ \mathbf{0} & \mathbf{P}_2 + \sigma\mathbf{Q}_2 \end{bmatrix}, \tag{19}$$

where $\sigma = \Re(s) \geq 0$. Since matrices $\mathbf{P}_1$, $\mathbf{P}_2$, $\mathbf{Q}_1$ and $\mathbf{Q}_2$ are all non-negative (Lemma 0), $\mathbf{W} + (\mathbf{W}^*)^T$ is therefore non-negative. Thus, the matrix $\mathbf{Y}(s)$ being positive-real, the HCFD-based modeling for single interconnect preserves passivity.

The discrete model of multi-conductor interconnects (MTL) can be straightforwardly obtained by extending the above formalization of the single interconnect (STL) and also the passivity of the MTL can be guaranteed.

Once the passive discrete modeling is available, one can calculate every poles of the impedance matrix, and incorporate the poles into a simulator. Another alternative is to directly use the obtained linear equations Eqns. 9 and 10. An advantage of the latter is that it is compatible with the available reduced-order algorithm and the Krylov subspace techniques for circuit reduction, and the further reduced-order model can be potentially obtained. However, in this paper we will not cover the issue of reduction, and we will simply use Eqns. 9 and 10 to obtain numerical results and observe the modeling efficiency.

IV. NUMERICAL RESULTS

Referring to the criterion adopted by HSPICE [12], the maximum frequency of interest can be evaluated by

$$f_{max} = \frac{0.35}{t_r}, \tag{20}$$

where t_r is the rise time of the input waveform.

The resolution of the presented method is to segment the interconnect into $2N$ equal sections, where the sizes of the segment depend on the minimum wavelength in the spectrum. A heuristic rule of selecting N is to make N equal to twice the number of the minimum wavelength:

$$N = 2df_{max}, \tag{21}$$

where f_{max} is the maximum frequency and d is the length of the interconnect. Thus the number of segmented sections of the interconnect is

$$N_p = 2N = 4df_{max}, \tag{22}$$

Accordingly, the number of state variables of discrete modeling of a line with length d is

$$N_s = 2N + 3 = 4df_{max} + 3. \tag{23}$$

The *first* example is a single interconnect having the following PUL parameters: $l = 360\ nH/m$, $c = 100\ pF/m$, $r = 36\ \Omega/m$, and $g = 0.01\ S/m$. Assuming that the digital signal has rise time $50ps$, the maximum frequency of interest is calculated by Eqn.20 to be 7 GHz. As the phase velocity is determined by $v_p = 1/\sqrt{lc} = 5/3 \times 10^8\ m/s$, the minimum wavelength is approximately 2.4 cm. The applied input is a step voltage whose rise time is $50\ ps$. By Eqn. 22, the number of sections using the HCFD-based modeling is approximately calculated as 4, and by Eqn. 23 the number of state variables is 7. The analysis shows that the frequency response of this modeling gives accurate results within the band from 0 to more than 8GHz. The transient results are shown in Fig. 4, compared to the results of the Method of Characteristics (MMC). The results of the case in which the number of the sections is selected to be 6 is also shown. Noting that the interconnect in this example is an undistorted line, the transient simulation response calculated by MMC is the exact value if the round errors are ignored [13]. The rule to select the number of grid points following Eqns. 20-23 can give considerable accuracy.

The *second* example represents two parts of bus at different layers connected by vias, as shown in Fig. 5. The length of each of the two identical interconnects is 2.5 cm.

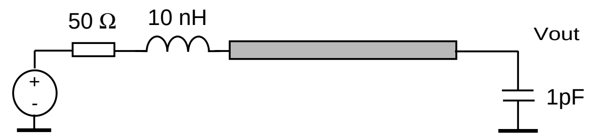

Fig. 3. Single interconnect.

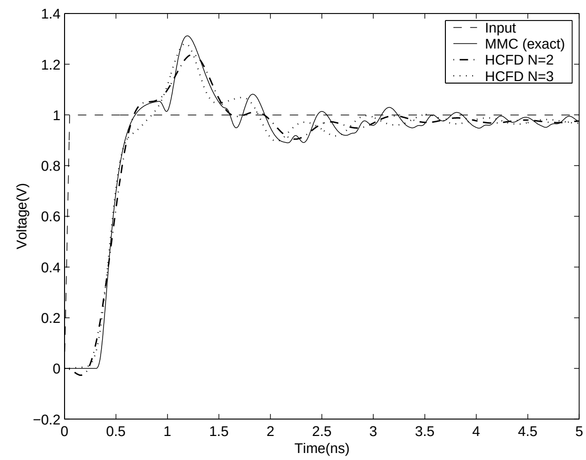

Fig. 4. Transient responses of single interconnect.

Using the rule that segments every minimum wavelength into 4 sections (Eqn.22), each of the interconnects is uniformly divided into 4 sections. The calculated waveforms of the main line at point A and the victim line at point B are shown in Figs. 6 and 6, respectively.

In this example, taking the same time step, the run time on an Ultra-1 SUN workstation by the HCFD-based modeling is 1.72 ns, including the initialization and read/write time, while that of FD in HSPICE is 6.5 ns. The run time is reasonable considering the fact that for the minimum wavelength, the presented modeling needs to segment it into only $2N = 4$ sections and totally generates $(2N+3)\times5\times2 = 70$ state variables, while FD in HSPICE needs 20 sections and totally generates $42 \times 5 \times 2 = 420$ state variables. This fact indicates that if the interconnect

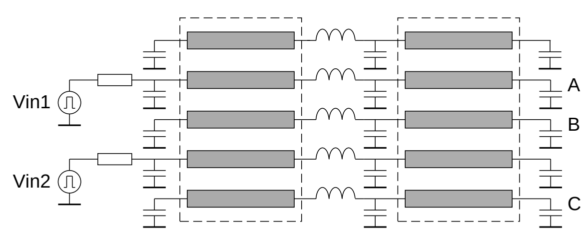

Fig. 5. Circuit of coupled interconnects.

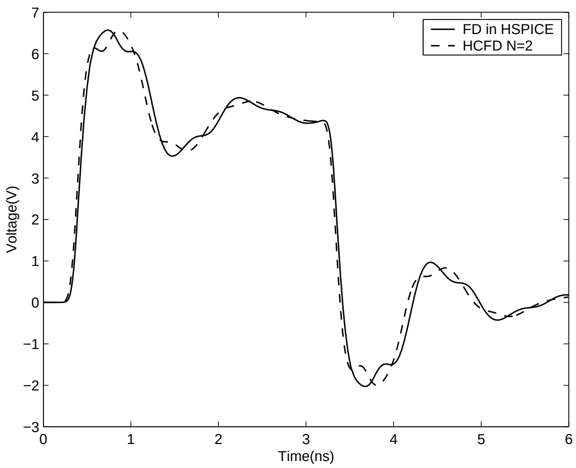

Fig. 6. Transient responses at A in Fig. 5.

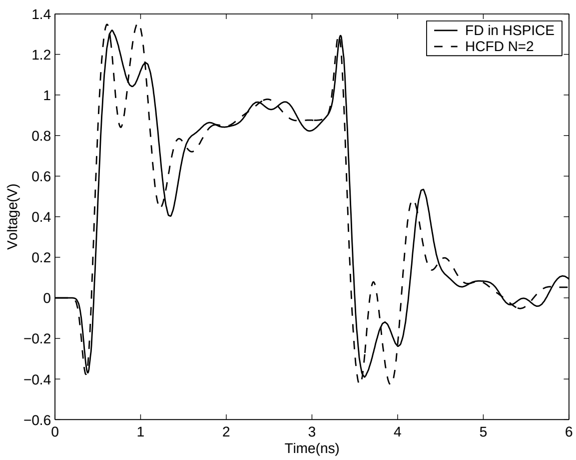

Fig. 7. Transient responses at B in Fig. 5.

circuit gets larger, the presented discrete modeling will gain more advantage over the FD-based modeling.

V. Conclusions

The high-order compact finite difference (HCFD) method is presented for passive discrete interconnect modeling, and the equivalent circuit model of interconnects is derived. The presented HCFD method discretizes the interconnect into few grid points across the entire length of the line and computes the electrical parameters at those points in order to derive accurate and efficient discrete approximation. The discrete approximation framework is determined by using Chebyshev polynomials. Like the FD modeling, the presented discrete modeling has explicit physical meaning, and results in equivalent circuits which can be directly incorporated into circuit simulators such as SPICE. Using the global approximation, the HCFD modeling is shown to produce highly accurate delay models, and can handle both single and multi-conductor interconnects. For the minimum wavelength of a single interconnect, the HCFD-based modeling generates 4 sections and 7 state variables as opposed to 20 sections and 42 states generated by FD in HSPICE. It is believed that the presented method gives higher approximation accuracy than other known passive discrete modeling taking the same number of state varibles. On the other hand, the HCFD-based modeling uses less grid points and less state variables, and generates much smaller though denser matrices than other FD-based methods to achieve the same accuracy. The interconnect modeling approach using high-order compact difference method preserves the passivity and generates fast solutions.

References

[1] L. T. Pillage and R. A. Rohrer, "Asymptotic waveform evaluation for timing analysis," *IEEE Trans. Computer-Aided Design*, vol. 9, no. 4, pp. 352–377, 1990.

[2] E. Chiprout and M. S. Nakhla, "Analysis of interconnect networks using complex frequency hopping," *IEEE Trans. Computer-Aided Design*, vol. 14, no. 2, pp. 186–200, 1995.

[3] P. Feldman and R. W. Freund, "Efficient linear circuit analysis by Pade approximation via the Lanczos process," *IEEE Trans. Computer-Aided Design*, vol. 14, no. 5, pp. 639–649, 1995.

[4] K. J. Kerns and A. T. Yang, "Stable and efficient reduction of large, multiport RC networks by pole analysis via congruence transformations," *IEEE Trans. Computer-Aided Design*, vol. 16, no. 7, pp. 734–744, 1997.

[5] A. Odabasioglu, M. Celik, and L. T. Pileggi, "PRIMA: Passive reduced-order interconnect macromodeling algorithm," *IEEE Trans Computer-Aided Design*, vol. 17, no. 8, pp. 645–653, 1998.

[6] A. C. Cangellaris, M. Celik, S. Pasha, and L. Zhao, "Electromagnetic model order reduction for system-level modeling," *IEEE Trans. Microwave Theory Tech.*, vol. 47, no. 6, pp. 840–849, 1999.

[7] C. Canuto, *Spectral methods in fluid dynamics*, New Youk: Springer-Verlag, 1988.

[8] M. Celik and A. C. Cangellaris, "Simulation of multiconductor transmission lines using Krylov subspace order-reduction techniques," *IEEE Trans. Computer-Aided Design*, vol. 16, no. 5, pp. 485–496, 1997.

[9] S. K. Lele, "Compact finite difference schemes with spectral-like resolution," *J. Comput. Phys.*, vol. 103, 1992.

[10] R. Bellman, B. G. Kashef, and J. Casti, "Differential quadrature: a technique for the rapid solution of nonlinear partial differential equations," *J. Comp. Phys.*, vol. 10, no. 1, pp. 40–52, 1972.

[11] R. W. Newcomb, *Linear Multiport Synthesis*, New York: McGraw Hill, 1966.

[12] Meta-Software, *HSPICE User's Manual*, Meta-Software, Inc, 1996.

[13] Q. Xu, Z. F. Li, P. Mazumder, and J. F. Mao, "Time-domain modeling of high-speed interconnects by modified method of characteristics," *IEEE Trans. Microwave Theory Tech.*, vol. 42, no. 2, pp. 323–327, 2000.